Improving Power Output of Battery and Mode Switching Frequency Based on Real-Time Average Power Method for Multi-Mode Hybrid Energy Storage System in Electric Vehicles

BIN WANG [ID][1,2], **QIAO HU**[1], **AND ZHIYU WANG**[1,2]

[1]State Key Laboratory for Manufacturing Systems Engineering, Xi'an Jiaotong University, Xi'an 710049, China
[2]Department of Mechanical Engineering, College of Engineering, University of Canterbury, Christchurch 8140, New Zealand

Corresponding author: Bin Wang (wangbin8751@xjtu.edu.cn)

ABSTRACT In this paper, a power-split strategy based on a real-time average power method is developed for improving power output of battery and mode switching frequency of a multi-mode hybrid energy storage system (HESS) in electric vehicles. To achieve mode switching and power distribution for the multi-mode HESS, a rule-based strategy is designed based on the high-frequency power demand. Furthermore, a simple real-time average power method is adopted to process the high-frequency power demand. Then, the real-time average power is used as a variable logic threshold value for the power-split strategy. Since the power-split controller responds to the smooth average power rather than the high-frequency power demand, the high-frequency mode switching of the multi-mode HESS can be avoided. The ultra-capacitor works as an enhanced low-pass power filter and the battery can supply smooth and steady output power to the motor inverter. Comparative simulations between the developed power-split strategy and the rule-based strategy are performed. The advantages of the developed power-split strategy for improving the power output of the battery and the mode switching frequency of the multi-mode HESS in electric vehicles are indicated under three typical driving cycles. Moreover, the longer time duration of the real-time average power is designed, the smoother power output of the battery and the lower mode switching frequency of the multi-mode HESS can be achieved.

INDEX TERMS Electric vehicles, battery, ultra-capacitor, hybrid energy storage system, power-split strategy, mode switching.

I. INTRODUCTION

Pure electric vehicles (EVs) have been considered as one of the most important parts in the sustainable transportation, due to their lower noise, lower carbon emission, and better economic performance when compared with traditional vehicles powered by internal combustion engines [1], [2]. For pure EVs, energy storage systems (ESSs) are of critical importance [3]. Generally, a battery pack is one of the most appropriate options for ESSs [4]. However, the battery cycle-life would be shortened with the high-frequency and

The associate editor coordinating the review of this manuscript and approving it for publication was Guijun Li [ID].

excessive power or current operation [5]. In other words, the energy management system (EMS) could not effectively deal with the high-frequency and excessive power operation in EVs if the ESS is only with the batteries [6], [7]. In practical applications, many series/parallel batteries could be used to enhance the power performance of the ESSs, while the mass, the size or the cost of these ESSs might not be satisfactory for EVs [8]. In addition, the energy management would become more difficult if more batteries need to be managed [9]. Ultra-capacitor (UC), as another one of the most appropriate options for the ESSs in EVs, has a significant high-power density and an excellent long charge-discharge cycle-life [10]. However, the drawback of the UC is that its

energy density is relatively low [11], [12]. So the UC can be used as an auxiliary energy source to integrate with the battery in a hybrid energy storage system (HESS), thereby achieving perfect high-power and high-energy performance, simultaneously [13].

In previous studies, HESSs were successfully used to avoid irregular current surge and prolong the battery cycle-life in EVs [1], [14]. Since the battery and the UC are used in the HESS, the energy management system (EMS) should effectively achieve power-split and coordinated usage between the two energy sources [15], [16]. To design the power-split strategy, the HESS topology should be considered firstly [17]. The topologies of HESSs include the passive-parallel topology [18], the semi-active topology [19], and the multi-mode topology [8]. The passive-parallel HESS cannot actively implement the power distribution between the two energy sources [18]. For the semi-active HESS, one of the two energy sources can be regulated with a DC/DC converter to supply optimal power, while the other is passively used to supply or absorb power [20]. Therefore, the semi-active HESS could not achieve the best usage of the battery or the UC. For the multi-mode HESS, it can work with various operating modes. These operating modes can be actively carried out [8], [13]. Moreover, both the battery and the UC can be actively controlled with a bidirectional DC/DC converter to implement the power distribution. In addition, the two energy sources can also individually supply power to the load without the bidirectional DC/DC converter, which can avoid the energy loss of the DC/DC conversion [21]. Therefore, the multi-mode HESS is a good choice to achieve the best usage of the battery or the UC.

Since various operating modes can be carried out for the multi-mode HESS, the power distribution between the two energy sources should be in accordance with these operating modes [22]. For this purpose, both the mode switching and the power distribution should be considered when designing the power-split strategy for the multi-mode HESS. Usually, the rule-based strategy can be employed to implement power distribution [23], [24]. According to different logic threshold values of the power demand, the voltage levels of the UC and the battery, the rule-based strategy can achieve a simple power-split control for the multi-mode HESS [8], [25]. However, the mode switching frequency might be very high if only the constant logic threshold values are utilized for the rule-based strategy [13]. These inflexible constant logic threshold values are not in accordance with the high-frequency power demand [26], [27]. To reduce the mode switching frequency, the hysteresis control (HC) method was proposed [28]. With the HC of the UC voltage and power levels, the power-split controller has buffer regions for the mode switching. However, the high-frequency power demand would pass through the HC region frequently such that the HC method might not restrain the high-frequency mode switching completely [13].

There are other optimization methods which can reduce the mode switching frequency [29], [30]. For instance,

the constant threshold values could be replaced by some variable logic threshold values for the rule-based strategy [31]. However, the rule-based strategy with many variable logic threshold values might be very complicated, i.e., many variable logic threshold values would involve the multi-level control for the EMS [32]. According to previous studies, some intelligent control methods such as the neural network [33] and the model predictive control [34] were developed to replace the rule-based strategy for the HESSs. But it is very difficult for developing controllers to implement the neural network and the model predictive control methods [34], [35]. To simplify the rule-based strategy with many variable logic threshold values, the real-time average power method (APM) could be used to process the high-frequency power demand [8], [27]. The real-time average power can be used as a variable and flexible logic threshold value for the power-split strategy. It can ensure that the battery can flexibly supply smooth and steady power to the load and the UC acted as an enhanced low-pass power filter needs to supply compensation power or absorb additional power [27], [36]. When the power-split controller responds to the smooth average power, the high-frequency mode switching of the multi-mode HESS can be avoided since the change frequency of the smooth average power is low [37]. Moreover, since the power output of the battery is designed according to the real-time average power rather than the high-frequency irregular power demand, the power output of the battery in the multi-mode HESS would be improved too.

In this paper, a power-split strategy based on a real-time APM is developed for the multi-mode HESS in EVs. It can effectively improve the power output of the battery and the mode switching frequency of the multi-mode HESS in EVs. Besides, the developed power-split strategy can be simply implemented. This paper is structured as below. Section 2 illustrates the multi-mode HESS. In Section 3, the rule-based strategy is developed. Section 4 presents the developed power-split strategy. Section 5 performs the simulations and the corresponding analyses. Section 6 presents the conclusions.

II. MULTI-MODE HESS

Fig. 1(a) illustrates the multi-mode HESS. It adopts a bidirectional DC/DC converter to interface the two energy sources. The UC interfaces the motor inverter directly such that it can work as an enhanced low-pass power filter, i.e., the UC can supply the compensation power or absorb the extra power frequently. With this topology, the battery can supply an optimal and steady output power to the UC or the motor inverter. Battery cycle-life can be extended due to the optimal smooth and steady output power operation. Moreover, the battery is always isolated from the load. To actively control the power flow transmission, two switches S1 and S2 are installed in the paths of the power flow transmission of the two energy sources. S1 and S2 are MOSFET switches, which can be controlled by the high logic signal (high or low voltage) and has a long lifetime. It can be seen that two reverse biased
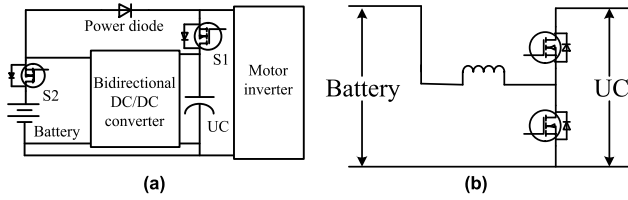
FIGURE 1. Configuration of the multi-mode HESS. (a) Multi-mode HESS; (b) Buck-boost converter.
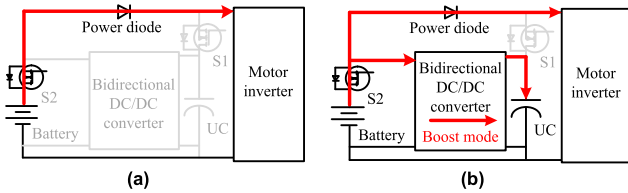

FIGURE 2. Operating modes with the UC/Battery scheme. (a) Pure battery driving mode; (b) Low power driving and recharging mode.

FIGURE 3. Operating modes with the Battery/UC scheme. (a) Hybrid Battery/UC driving mode; (b) Pure UC driving mode.

FIGURE 4. Operating modes in braking condition. (a) Pure UC recover mode; (b) Hybrid UC/Battery recover mode.

power diodes are paralleled with S1 and S2, respectively. The recover power could be recovered through the power diodes if S1 or S2 is turned OFF. Notice that, the minimum operating voltage of the UC is higher than the battery output voltage. The bidirectional DC/DC converter should operate with boost mode when the power flow transmission is from the battery to the UC. On the contrary, when the power flow transmission is from the UC to the battery, the bidirectional DC/DC converter should operate with buck mode. As shown in Fig. 1(b), the bidirectional DC/DC converter is a buck-boost converter.

When driving the EV, the multi-mode HESS has four operating modes to supply power. If S1 is turned OFF and S2 is turned ON, the UC/Battery scheme could be actively implemented. With this operating scheme, the multi-mode HESS has two operating modes, as shown in Fig. 2. For the pure battery driving mode, it has no energy to flow the buck-boost converter. So this operating mode can avoid the DC/DC energy consumption. For the low power driving and recharging mode, the battery needs to supply a low power to the motor inverter. The UC doesn't need to supply power, and the buck-boost converter should operate with the boost mode to charge the UC.

When S1 is turned ON, the power diode would be reverse biased. In this case, the Battery/UC scheme can be actively implemented. With this operating scheme, the multi-mode HESS also has two operating modes, as illustrated in Fig. 3. If S2 is turned ON, the hybrid Battery/UC driving mode could be actively carried out and the buck-boost converter should work with the boost mode. The battery can supply power with the buck-boost converter. With this operating mode, the UC works as a low-pass power filter. If S2 is turned OFF, the pure UC driving mode can be activated. With this operating mode, the buck-boost converter doesn't need to work. The UC has too much energy such that it has a priority to supply power.

During the regenerative braking, both S1 and S2 are turned OFF. The braking power can be recovered through the power
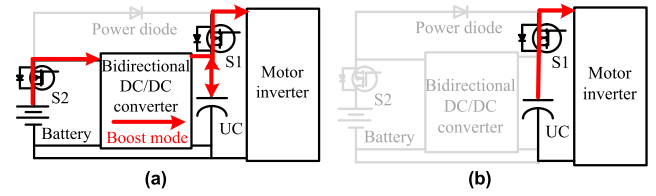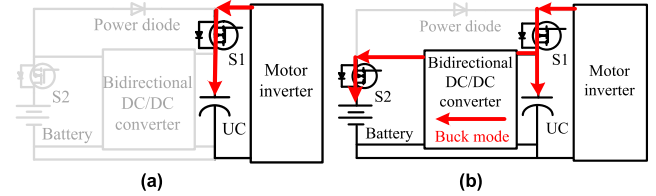
diode paralleled with the switch S1. As shown in Fig. 4, two operating modes can be implemented based on the ON/OFF state of the buck-boost converter. In general, the buck-boost converter is turned OFF since the UC has the priority to recover the braking energy. However, if the UC is fully charged, the buck-boost converter should work with the buck mode to charge the battery. In this case, the power can be recovered through the power diode paralleled with the switch S2. To prolong the battery cycle-life, the constant current control should be implemented for the buck-boost converter.

Based on the specific configuration of the multi-mode HESS, six operating modes can be implemented. So the mode switching of the six operating modes and the corresponding power distribution in different operating modes should be taken into account for the design of the power-split strategy. In the next sections, the rule-based strategy will be firstly designed. Then, we will improve the rule-based strategy and develop a power-split strategy based on the real-time APM.

III. RULE-BASED STRATEGY
A. MODE SELECTION AND MODE SWITCHING
The rule-based strategy uses some constant logic threshold values to actively select the operating modes of the multi-mode HESS in accordance with the power demand, the UC voltage, and the battery voltage/SOC, as shown in Fig. 5.

The constraints for the voltage of the battery and the UC should be satisfied when starting the EV.

$$V_{\text{battery}} > V_{\text{battery}}^{\text{low}} \tag{1}$$

$$V_{\text{UC}} > V_{\text{battery}} \tag{2}$$

where $V_{\text{battery}}^{\text{low}}$ is the low limit of the battery voltage, which is in accordance with the state of charge $SOC_{\text{battery}}^{\text{low}} = 0.1$.

During the regenerative braking, the pure UC recover mode should be selected when the UC voltage is lower than the up limit (95% of its rated voltage). However, if the EV has a long duration of the braking condition, the UC
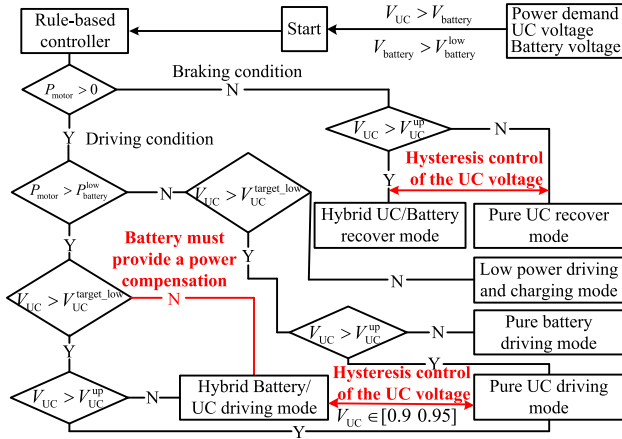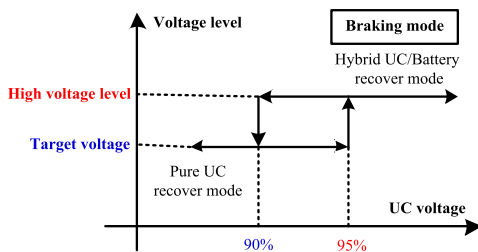
FIGURE 5. Mode selection and mode switching.

FIGURE 6. HC in braking mode.

FIGURE 7. HC in driving mode.

method, the UC can supply enough power to meet the high power demand. Meanwhile, the system stability can be guaranteed. Furthermore, the power level should be defined for designing the mode switching rules among the low power driving and recharging mode, the pure battery driving mode and the hybrid Battery/UC driving mode. To prevent the high-frequency mode switching among the three operating modes, a 2000 W power of HC region is also designed to implement the mode switching according to the engineering experiences. The HC of the UC voltage and power level are designed as Fig. 7. The low limit of the HC power region is designed as 1000 W. So the up limit of the HC power region is 3000 W.

B. POWER DISTRIBUTION

When the pure UC driving mode or the pure battery driving mode is implemented, the output power of the buck-boost converter is equal to zero. The power distribution of the pure UC driving mode or the pure battery driving mode is defined as (3) and (4), respectively.

$$P_{\text{bat}}^{\text{dem}} = 0 \ \& \ P_{\text{UC}}^{\text{dem}} = P_{\text{motor}}^{\text{dem}} \tag{3}$$

$$P_{\text{bat}}^{\text{dem}} = P_{\text{motor}}^{\text{dem}} \ \& \ P_{\text{UC}}^{\text{dem}} = 0 \tag{4}$$

where $P_{\text{bat}}^{\text{dem}}$, $P_{\text{UC}}^{\text{dem}}$ represent the power demand of the battery and the UC, respectively. $P_{\text{motor}}^{\text{dem}}$ represents the power demand from the motor inverter.

On the other hand, the battery must supply all the power to the load when the low power driving and recharging mode is used. With this operating mode, the battery should charge the UC with constant power by using the buck-boost converter. To obtain a high working efficiency of the multi-mode HESS, the buck-boost converter should work with the optimum efficiency.

$$P_{\text{bat}}^{\text{dem}} = P_{\text{motor}}^{\text{dem}} + P_{\text{dc\_input}}^{\text{peak\_efficiency}} \ \& \ P_{\text{UC}}^{\text{dem}} = -P_{\text{dc\_output}}^{\text{peak\_efficiency}} \tag{5}$$

where $P_{\text{dc\_input}}^{\text{peak\_efficiency}}$, $P_{\text{dc\_output}}^{\text{peak\_efficiency}}$ are the input and output power when the buck-boost converter is working with the optimum efficiency, respectively.

When the hybrid Battery/UC driving mode is used, the power distribution includes two situations. Usually, the battery provides the constant power with the buck-boost converter, and the UC should supply the additional power. To improve the operating efficiency, the buck-boost converter

would be fully charged. To ensure the UC safety, the hybrid UC/Battery recover mode would be selected if the UC voltage is higher than the up limit. To reduce the mode switching frequency between the pure UC recover mode and the hybrid UC/Battery recover mode, the HC of the UC voltage is designed for the braking mode. Notice that, 90% of the UC rated voltage is the target voltage, as shown in Fig. 6.

In driving conditions, the power demand is positive. If the power demand is lower than the low power limit (i.e., $P_{\text{motor}} < P_{\text{battery}}^{\text{low}}$) and the UC voltage is lower than the low-target voltage (i.e., $V_{\text{UC}} \leq V_{\text{UC}}^{\text{target\_low}}$, in which $V_{\text{UC}}^{\text{target\_low}}$ is equal to 71% of its rated voltage), the low power driving and recharging mode should be selected. With this design, the UC would have enough energy to feed the motor inverter at the later high power demand. When the UC voltage is in the normal target voltage region (i.e., $V_{\text{UC}}^{\text{target\_low}} \leq V_{\text{UC}} \leq V_{\text{UC}}^{\text{up}}$), if $P_{\text{motor}} < P_{\text{battery}}^{\text{low}}$, the pure battery driving mode can be used. However, if $V_{\text{UC}} > V_{\text{UC}}^{\text{up}}$, to guarantee that the UC can absorb the braking energy at the later braking condition, the pure UC driving mode must be actively implemented to discharge the UC. In addition, if $P_{\text{motor}} \geq P_{\text{battery}}^{\text{low}}$ and $V_{\text{UC}} \leq V_{\text{UC}}^{\text{up}}$, the hybrid Battery/UC driving mode should be implemented.

Similarly with Fig. 6, the HC design of UC voltage can be used to avoid the high-frequency mode switching among the pure UC driving mode, the hybrid Battery/UC driving mode and the pure battery driving mode. By using the HC
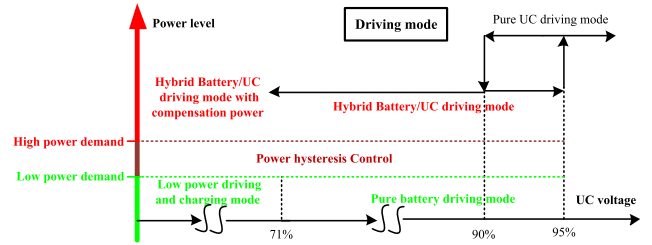
also works at the optimum efficiency.

$$P_{\text{bat}}^{\text{dem}} = P_{\text{dc\_input}}^{\text{peak\_efficiency}} \quad \& \quad P_{\text{UC}}^{\text{dem}} = P_{\text{motor}}^{\text{dem}} - P_{\text{dc\_output}}^{\text{peak\_efficiency}} \quad (6)$$

In particular, if $V_{\text{UC}} \leq V_{\text{UC}}^{\text{target\_low}}$ or the power demand is high, the battery should provide compensation power to the motor inverter. For instance, if the UC voltage is equal to 50% of its rated voltage, it has little power to feed the motor inverter such that the battery should supply the maximum compensation power. The maximum compensation power should be designed according to the maximum output power of the buck-boost converter. For the compensation control, the power demand of the battery in (6) is changed as.

If $P_{\text{motor}}^{\text{dem}} > P_{\text{bat}}^{\text{constant}}$,
$$P_{\text{bat}}^{\text{dem}} = P_{\text{bat\_1}}^{\text{dem}} = (P_{bat}^{\text{max}} - P_{\text{bat}}^{\text{constant}})$$
$$\times \frac{(P_{\text{motor}}^{\text{dem}} - P_{\text{bat}}^{\text{constant}})}{P_{\text{dem}}^{\text{max}} - P_{\text{bat}}^{\text{constant}}} + P_{\text{bat}}^{\text{constant}} \quad (7)$$

If $V_{\text{UC}}^{\text{target\_low}} > V_{\text{UC}}$,
$$P_{\text{bat}}^{\text{dem}} = P_{\text{bat\_2}}^{\text{dem}} = (P_{bat}^{\text{max}} - P_{\text{bat}}^{\text{constant}})$$
$$\times \frac{(V_{\text{UC}}^{\text{target\_low}} - V_{\text{UC}})}{(V_{\text{UC}}^{\text{target\_low}} - 0.5)} + P_{\text{bat}}^{\text{constant}} \quad (8)$$

If $P_{\text{motor}}^{\text{dem}} > P_{\text{bat}}^{\text{constant}} \ \& \ V_{\text{UC}}^{\text{target\_low}} > V_{\text{UC}}$,
$$P_{\text{bat}}^{\text{dem}} = \max(P_{\text{bat\_1}}^{\text{dem}}, P_{\text{bat\_2}}^{\text{dem}}) \quad (9)$$

where $P_{\text{bat}}^{\text{max}}$ represents the maximum output power of the battery; $P_{\text{dem}}^{\text{max}}$ is equal to the maximum power demand from the motor inverter; $P_{\text{bat}}^{\text{constant}}$ is equal to $P_{\text{dc\_input}}^{\text{peak\_efficiency}}$.

With the logic threshold values and the HC method, the mode selection and the corresponding power distribution can be achieved. However, these threshold values are static values, while the power demand is high-frequency. So the rule-based controller cannot dynamically achieve the mode selection and power distribution for the multi-mode HESS in accordance with the high-frequency power demand.

IV. POWER-SPLIT STRATEGY BASED ON THE REAL-TIME APM

As mentioned above, if the mode switching responds to the high-frequency power demand directly, the mode switching frequency might be very high. It would affect the system stability of the multi-mode HESS. What's worse, the power output of the battery would be high-frequency, which would shorten the battery cycle-life. To improve the rule-based strategy, the real-time APM is proposed to process the high-frequency power demand. The real-time average power will be utilized as one of the variable logic threshold values to implement the mode switching and power distribution. Since the real-time average power is variable and follows the power demand, the mode switching and power distribution would become flexible and reliable.

Generally, the future power demand is very difficult to predict since it is determined by the driving cycles and the driver's intended actions. For the APM, the real-time average
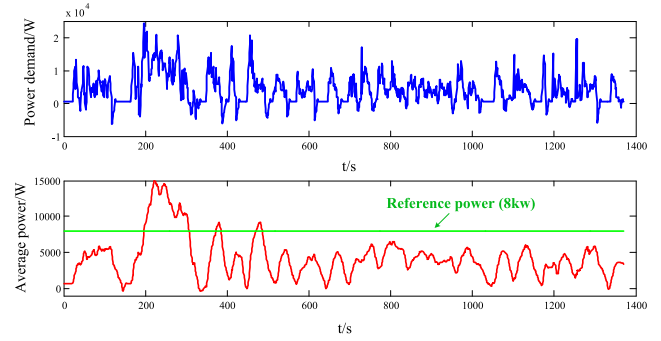

FIGURE 8. Real-time average power in the UDDS.

power is obtained according to the historic power and real-time power demands.

$$\begin{cases} P_{\text{ave}} = (\int_t^{t+T_s} P_{\text{dem}} dt)/T_s, & t \geq T_s \\ P_{\text{ave}} = (\int_0^t P_{\text{dem}} dt)/t, & 0 < t < T_s \end{cases} \quad (10)$$

where T_s is the time duration.

The above APM is quite simple but effective. For instance, the real-time average power with 30 s of time duration in the Urban Dynamometer Driving Schedule (UDDS) is shown in Fig. 8. It can be obviously seen that the real-time average power is smoother than the power demand. So the power-split strategy is developed according to the real-time average power and the rule-based strategy. Actually, the developed power-split strategy is an improved rule-based strategy.

In braking conditions, the mode switching and power distribution of the developed power-split strategy are the same as the rule-based strategy. In the driving condition, the power-split strategy based on the real-time APM is designed as follows.

A. PURE UC DRIVING MODE
The energy management (i.e., mode selection and power distribution) is the same as the aforementioned rule-based strategy.

B. PURE BATTERY DRIVING MODE
The power distribution is the same as the aforementioned rule-based strategy. However, the restrictive condition of the mode selection is changed. The real-time average power is used as a variable logic threshold value for the power-split strategy. Furthermore, the optimum efficiency point of the buck-boost converter is designed as a reference power (i.e., $P_{\text{reference}} = P_{\text{dc\_input}}^{\text{peak\_efficiency}}$). When the UC voltage is in the normal target voltage region, if the reference power is higher than the real-time average power (i.e., $P_{\text{reference}} > P_{\text{ave}}$) and $P_{\text{motor}} < P_{\text{battery}}^{\text{low}}$, the pure battery driving mode will be implemented.

C. HYBRID BATTERY/UC DRIVING MODE
The energy management is totally different from the aforementioned rule-based strategy. When the UC voltage is in the

normal target voltage region and the power demand is higher than the low power limit, if $P_{\text{reference}} < P_{\text{ave}}$, the hybrid Battery/UC driving mode should be selected. The power output of the battery is designed according to the real-time average power. The UC supplies or absorbs the extra power, as shown in (11).

$$P_{bat}^{\text{dem}} = P_{\text{ave}}/\eta_{\text{dc}} \ \& \ P_{\text{UC}}^{\text{dem}} = P_{\text{motor}}^{\text{dem}} - P_{\text{ave}} \qquad (11)$$

where η_{dc} represents the working efficiency of the buck-boost converter.

If $P_{\text{reference}} > P_{\text{ave}}$, the battery only provides the constant reference power with the buck-boost converter. The UC should absorb the extra power.

$$P_{bat}^{\text{dem}} = P_{\text{reference}}/\eta_{\text{dc}} \ \& \ P_{\text{UC}}^{\text{dem}} = P_{\text{motor}}^{\text{dem}} - P_{\text{reference}} \qquad (12)$$

When the UC voltage is lower than the low-target voltage, the stored energy in the UC would be less than 50%. The UC energy should be compensated with the hybrid UC/battery driving mode. The compensation power of the battery is

$$P_{bat}^{\text{dem}} = (P_{bat}^{\text{max}} - P_{\text{ave/ref}}) \frac{(V_{\text{UC}}^{\text{target\_low}} - V_{\text{UC}})}{(V_{\text{UC}}^{\text{target\_low}} - 0.5)} + P_{\text{ave/ref}} \qquad (13)$$

where $P_{\text{ave/ref}} = \max\{P_{\text{ave}}, P_{\text{reference}}\}$.

D. LOW POWER DRIVING AND RECHARGING MODE

The energy management is the same as the aforementioned rule-based strategy.

For the developed power-split strategy, the same HC of the UC voltage and the power levels are also used to reduce the mode switching frequency. Moreover, the real-time APM is used to improve the mode switching frequency, which is an enhanced constraint for avoiding the high-frequency mode switching. Besides, the power-split strategy can effectively improve the power output of the battery by using the real-time APM.

V. RESULTS AND DISCUSSION

To validate the developed power-split strategy for the multi-mode HESS, a simulation model is established in Simulink, as shown in Fig. 9. Table 1 shows the related parameters. The mode switching and the power distribution of the multi-mode HESS will be discussed in three driving cycles, i.e., the UDDS, the New York City Cycle (NYCC), and the New European Driving Cycle (NEDC).

The power demand and the real-time average power of the NYCC and the NEDC are shown in Fig.10. In the NYCC, the reference power is always higher than the real-time average power. So the battery only needs to supply the constant power when the hybrid Battery/UC driving mode is used. In the NEDC, although the real-time average power is higher than the reference power at sometimes, it is smoother and lower than the power demand. Notice that, the real-time average power will be higher than 20 kW. In this condition, the battery would supply the maximum power to the motor inverter.
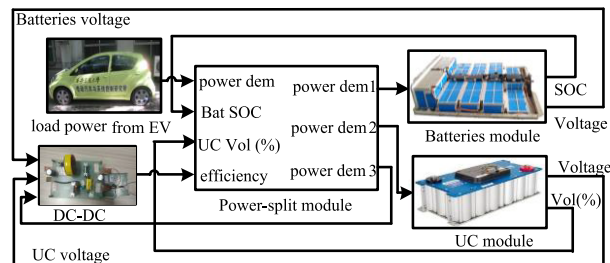

FIGURE 9. Simulation model.

TABLE 1. Important parameters of the simulation model.

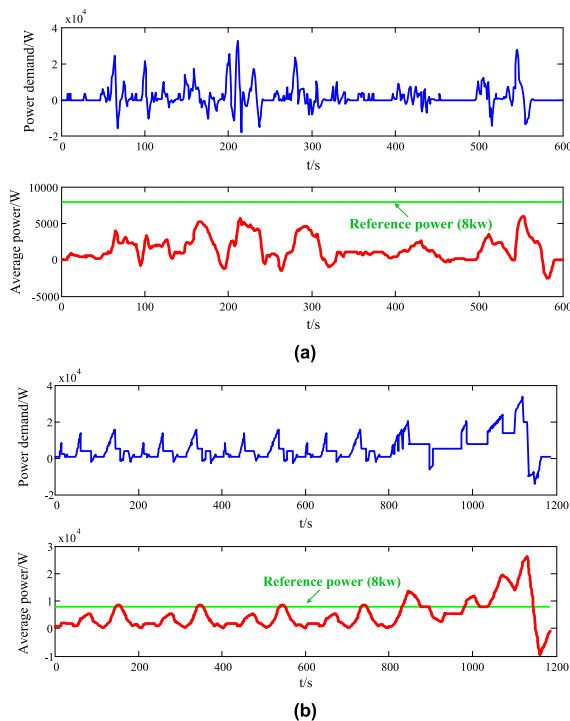|	
Total mass of the EV	750Kg
Vehicle Motor	20kW
UC pack	400V 16F
Battery pack	300V 40Ah
Bidirectional DC/DC converter	Peak efficiency: 8kW
Accessory power	500W

(a)

(b)

FIGURE 10. Real-time average power in the NYCC and the NEDC. (a) NYCC; (b) NEDC.

The comparison of the two strategies in the UDDS is illustrated in Fig. 11. With the developed power-split strategy, the high-frequency power output of the battery can be avoided. Usually, the power output of the battery is constant when the hybrid Battery/UC driving mode is implemented. Meanwhile, the constant power can be designed in accordance with the optimum power output of the battery and the optimum efficiency of the buck-boost converter. So the
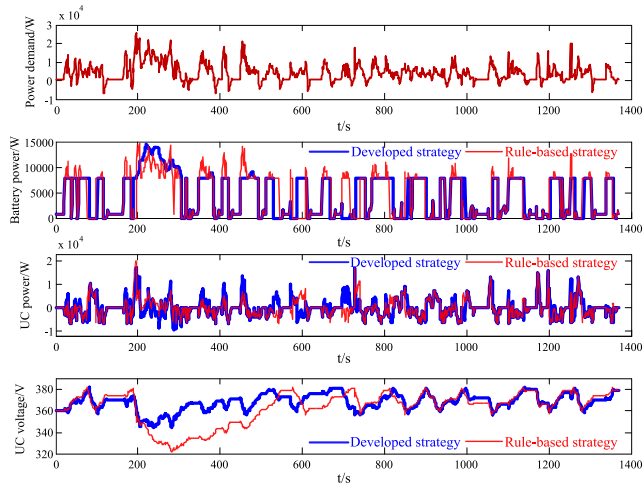
FIGURE 11. Comparison between the two strategies in the UDDS.

FIGURE 12. Comparison between the two strategies in the NYCC.

battery cycle-life can be extended and the working efficiency of the multi-mode HESS can be improved, simultaneously. However, with the rule-based strategy, the change frequency of the corresponding power output of the battery is very high, which would shorten the battery cycle-life.

On the other hand, the mode switching can be implemented based on the battery and the UC power profiles. For instance, when the battery power is higher than 8 kW and the UC power is higher than zero, the hybrid Battery/UC driving mode is implemented. While the battery power is less than 3 kW and the UC power is equal to zero, the operating mode is switched to the pure battery driving mode. When the battery power is equal to zero and the UC power is higher than zero, the operating mode is switched to the pure UC driving mode. It can be known that mode switching frequency can be reduced based on the developed power-split strategy. It is without a doubt, the low mode switching frequency can enhance the system stability of the multi-mode HESS.

The comparative results in Fig. 11 also show the control effect of the power compensation of the two strategies. With the developed power-split strategy, the power compensation control is only used when the power demand is very high. Moreover, the compensation power of the battery increases smoothly. However, the power compensation control is usually used when the rule-based strategy is implemented. What's worse, the compensation power increases suddenly, which would be harmful to the battery cycle-life. Based on the UC voltage profile, it can be known that UC is deeply discharged with the rule-based strategy. The corresponding voltage is 320 V∼380 V after 200 s. Compared with the rule-based strategy, the UC works as an enhanced low-pass power filter and is charged/discharged more frequently within the voltage of 340 V∼380 V with the developed power-split strategy. Although the real-time APM has a delay effect, the UC will provide additional power such that the battery can supply the smooth and steady output power. For the HESS, the smooth increase of the output power would be
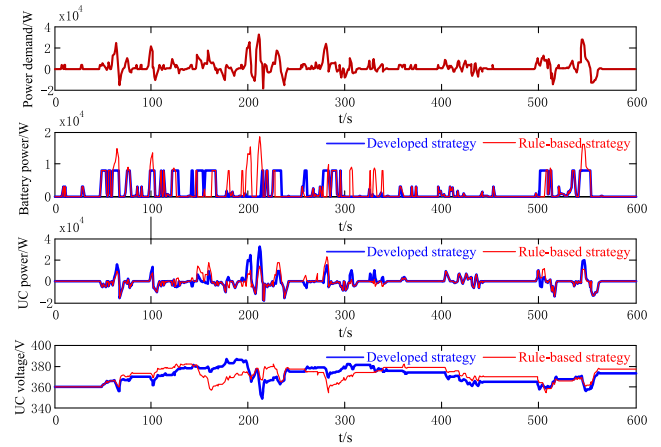
more suitable and acceptable for the stability control of the EMS. Furthermore, the developed power-split strategy can guarantee that the battery provides low output power, the low-frequency and constant power in most cases. The low output power, the low-frequency and constant output power have a less adverse effect for the battery cycle-life when compared with the high-frequency and peak-value output power.

The comparative results in the NYCC are shown in Fig. 12. The same pure battery driving modes are used with the two strategies at the start, since the power demand is less than the low power level and the UC voltage is equal to 90% of its rated voltage. By combining with Fig. 10(a), it can be known that the reference power is always higher than the real-time average power in the NYCC. So the battery never needs to supply compensation power with the developed power-split strategy. Moreover, the buck-boost converter can work with peak efficiency when the hybrid Battery/UC driving mode is implemented. While the rule-based strategy is used, it increases the mode switching frequency. The battery responds to the excessive power demand around 200 s such that it provides sudden compensation power when the hybrid Battery/UC driving mode is implemented. Although the compensation power can respond to the peak-power demand rapidly, this operation might affect the system stability of the multi-mode HESS. In practical applications, engineers do not encourage to use this operation since it has an adverse effect on the battery cycle-life.

In both the UDDS and the NYCC, the developed strategy has a delay effect to avoid the battery providing excessive power or sudden increased power to the motor inverter. So the battery power output becomes smoother than the rule-based strategy. If the battery supplies the optimal smooth and steady output power with the hybrid Battery/UC driving mode, the UC would supply more compensation power or absorb more extra power. So the UC would work as an enhanced low-pass power filter to extend the battery cycle-life.

Also, the control effect of the two strategies in the NEDC is performed, as shown in Fig. 13. Since the change frequency of

TABLE 2. Quantitative evaluation of the two strategies.

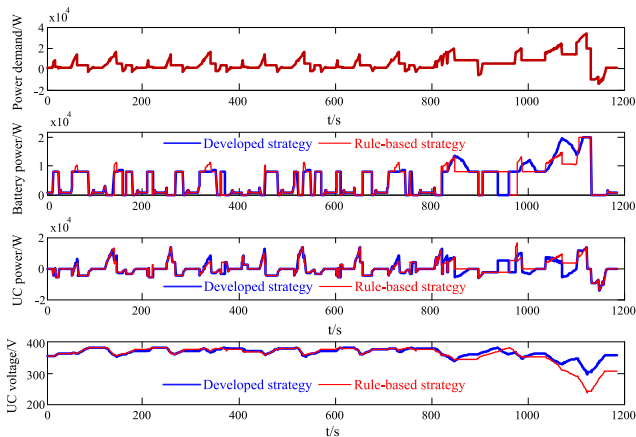| Driving cycles	Energy loss in buck-boost converter		Total energy consumption		System working efficiency	
	Developed strategy	Rule-based strategy	Developed strategy	Rule-based strategy	Developed strategy	Rule-based strategy
UDDS	15.6 kJ	17.4 kJ	6328.7 kJ	6419.9 kJ	91.73%	90.42%
NYCC	13.2 kJ	16.2 kJ	989.5 kJ	1000.3 kJ	90.26%	89.28%
NEDC	11.4 kJ	11.4 kJ	6260. 4 kJ	6281.7 kJ	92.33%	92.02%

FIGURE 13. Comparison between the two strategies in the NEDC.

the power demand based on the NEDC is very low, the mode switching frequency of the two strategies has no significant difference. The obvious difference between the two strategies is the power compensation when the power demand is high after 1050 s. With the developed power-split strategy, the battery can provide enough compensation power to charge the UC after 1050 s due to the reference power is lower than the real-time average power. The UC voltage can be maintained up to 300 V. As a comparison, with the rule-based strategy, the UC drops quickly after 1050 s, while the battery cannot provide enough compensation power to charge the UC since the compensation power is designed according to the actual power demand. Then, the UC voltage is lower than 284 V, the battery needs to supply more power. However, the maximum power of the battery output is 20 kW such that the UC voltage cannot be effectively recovered with the rule-based strategy. Meanwhile, the compensation power of the battery also increases suddenly.

Based on the above analyses, it can be known that the battery should supply the compensation power with a slight delay with the developed power-split strategy. In EV applications, the UC energy design can guarantee that it can supply high output power within 30 s. It allows a suitable delay for the compensation power control of the battery. However, the power compensation control is directly implemented with the rule-based strategy when the power demand is high. So the power output of the battery increases suddenly. What's worse, the UC energy might not be compensated effectively.
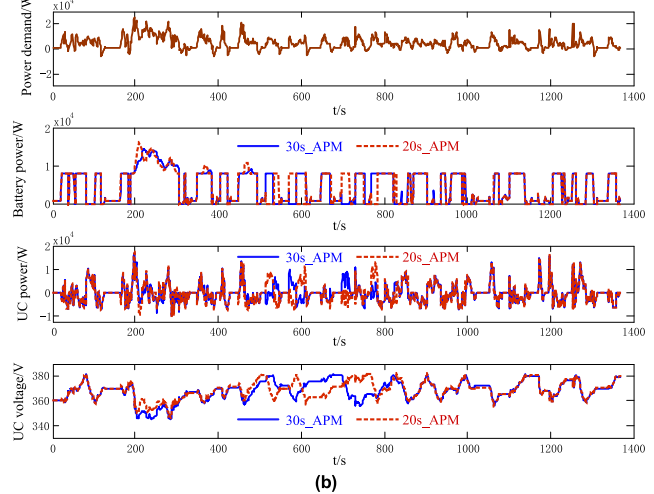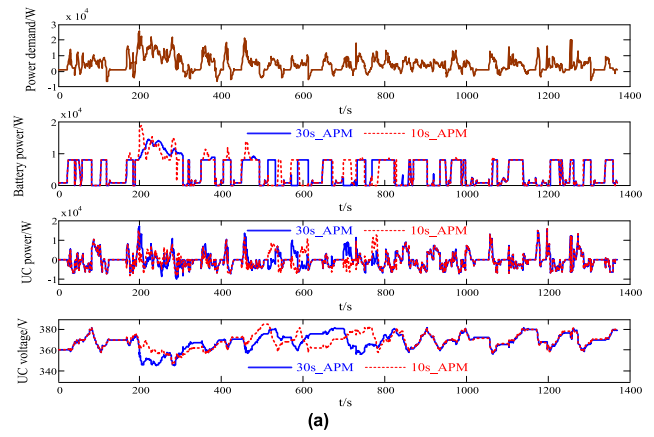

FIGURE 14. Comparative analyses in the UDDS. (a) Comparison between the 30s_APM and the 10s_APM; (b) Comparison between the 30s_APM and the 20s_APM.

The quantitative evaluation of the two strategies based on different driving cycles is illustrated in Table 2. Since the extra energy dissipation cannot be avoided with the ON/OFF state switching of the buck-boost converter, the lower frequency of the mode switching is obtained, the more energy can be saved. Therefore, the developed power-split strategy would improve the working efficiency of the multi-mode HESS. Compared to the rule-based strategy, the developed power-split strategy can improve the system working efficiency up to 1.31% and 0.98% in the UDDS and the NYCC, respectively. In the NEDC, the system working efficiency

is not significantly improved with the developed power-split strategy, since the mode switching of the two strategies has no significant difference.

It is known that the developed power-split strategy has a delay effect on the power compensation control of the battery. So the power compensation control based on different time durations of the real-time average power is also studied. The time durations are designed as $T_s = 10s$, $T_s = 20s$, and $T_s = 30s$, respectively. We define them as 10s_APM, 20s_APM, and 30s_APM, respectively. The comparative results are illustrated in Fig. 14. The significant difference is that the power compensation control would be carried out in advance when the 10s_APM or the 20s_APM is implemented. If the 10s_APM is implemented, the mode switching frequency would increase obviously. What's worse, the peak power of the battery is close to 20 kW after 200 s, which would be harmful to the battery cycle-life. While the 20s_APM is implemented, both the mode switching frequency and the peak power of the battery can be improved. Actually, the longer time duration is designed, the smoother for the real-time average power can be achieved. However, the time duration design of the real-time average power should consider the maximum stored energy of the UC. Compared with the 30s_APM, although the battery could provide the power compensation earlier if the 10s_APM or the 20s_APM is implemented, the power output of the battery and the mode switching frequency of the multi-mode HESS would become worse.

VI. CONCLUSION

This paper has developed a power-split strategy based on a real-time APM for improving the power output of the battery and the mode switching frequency of the multi-mode HESS in EVs. The rule-based strategy was firstly designed to achieve the mode selection and power distribution. Then, a simple real-time APM was developed to deal with the high-frequency power demand. On this basis, the power-split strategy was developed based on the real-time average power. With this design, the UC can work as an enhanced low-pass power filter. The high-frequency mode switching can be avoided since the multi-mode HESS responds to the smooth average power rather than the high-frequency power demand. Moreover, the power output of the battery and the system stability of the multi-mode HESS can be improved, simultaneously.

Numerous analyses based on three driving cycles were presented to validate the developed power-split strategy. In the UDDS and the NYCC, the developed power-split strategy can effectively improve the mode switching frequency of the multi-mode HESS. Furthermore, the developed power-split strategy has a delay effect to prevent the battery from providing the excessive power to the motor inverter. So the power output of the battery becomes smooth. Since the battery usually operates with a suitable constant power or optimal smooth power, the battery cycle-life can be extended. In addition, the advantage of power compensation control

based on the developed power-split strategy is obvious. The power compensation of battery based on the rule-based strategy increases suddenly, while it is with a smooth increase with the developed power-split strategy. Compared with the UDDS and the NYCC, this advantage is more obvious in the NEDC. It is without a doubt, the smooth power compensation control can enhance the system stability of the multi-mode HESS.

In addition, this paper also studied the power compensation control effect based on different time durations of the real-time average power. Results showed that the longer time duration was designed, the smoother real-time average power and the better mode switching of the multi-mode HESS could be achieved. However, the UC should supply more extra power to compensate the battery power output when the time duration of the real-time average power was added. Therefore, the time duration design of the real-time average power should consider the maximum stored energy of the UC. According to the comparative analyses, it can be known that the power-split strategy with the 30s_APM could achieve the satisfied control effect of the mode switching and smooth power output of the battery for the multi-mode HESS. In EV applications, the smooth power output of the battery would be very useful for extending the battery cycle-life.

REFERENCES

[1] M. A. Hannan, M. M. Hoque, A. Mohamed, and A. Ayob, "Review of energy storage systems for electric vehicle applications: Issues and challenges," *Renew. Sustain. Energy Rev.*, vol. 69, pp. 771–789, Mar. 2017.

[2] E. Jiaqiang, G. Liu, Z. Zhang, D. Han, J. Chen, K. Wei, J. Gong, and Z. Yin, "Effect analysis on cold starting performance enhancement of a diesel engine fueled with biodiesel fuel based on an improved thermodynamic model," *Appl. Energy*, vol. 243, pp. 321–335, Jun. 2019.

[3] O. Veneri, C. Capasso, and S. Patalano, "Experimental investigation into the effectiveness of a super-capacitor based hybrid energy storage system for urban commercial vehicles," *Appl. Energy*, vol. 227, pp. 312–323, Oct. 2018.

[4] V. K. Kasimalla, G. N. Srinivasulu, and V. Velisala, "A review on energy allocation of fuel cell/battery/ultracapacitor for hybrid electric vehicles," *Int. J. Energy Res.*, vol. 42, no. 14, pp. 4263–4283, Nov. 2018.

[5] J. Li, A. M. Gee, M. Zhang, and W. Yuan, "Analysis of battery lifetime extension in a SMES-battery hybrid energy storage system using a novel battery lifetime model," *Energy*, vol. 86, pp. 175–185, Jun. 2015.

[6] R. Xiong, J. Cao, and Q. Yu, "Reinforcement learning-based real-time power management for hybrid energy storage system in the plug-in hybrid electric vehicle," *Appl. Energy*, vol. 211, pp. 538–548, Feb. 2018.

[7] Z. Song, J. Li, J. Hou, H. Hofmann, M. Ouyang, and J. Du, "The battery-supercapacitor hybrid energy storage system in electric vehicle applications: A case study," *Energy*, vol. 154, pp. 433–441, Jul. 2018.

[8] B. Wang, J. Xu, B. Cao, and X. Zhou, "A novel multimode hybrid energy storage system and its energy management strategy for electric vehicles," *J. Power Sources*, vol. 281, pp. 432–443, May 2015.

[9] K. S. Sandhu and A. Mahesh, "A new approach of sizing battery energy storage system for smoothing the power fluctuations of a PV/wind hybrid system," *Int. J. Energy Res.*, vol. 40, no. 9, pp. 1221–1234, Jul. 2016.

[10] P.-H. Huang, J.-K. Kuo, and C.-Y. Huang, "A new application of the UltraBattery to hybrid fuel cell vehicles," *Int. J. Energy Res.*, vol. 40, no. 2, pp. 146–159, Feb. 2016.

[11] L. Sun, P. Walker, K. Feng, and N. Zhang, "Multi-objective component sizing for a battery-supercapacitor power supply considering the use of a power converter," *Energy*, vol. 142, pp. 436–446, Jan. 2018.

[12] J. Meng, D.-I. Stroe, M. Ricco, G. Luo, and R. Teodorescu, "A simplified model-based state-of-charge estimation approach for lithium-ion battery with dynamic linear model," *IEEE Trans. Ind. Electron.*, vol. 66, no. 10, pp. 7717–7727, Oct. 2019.

[13] B. Wang, J. Xu, R.-J. Wai, and B. Cao, "Adaptive sliding-mode with hysteresis control strategy for simple multimode hybrid energy storage system in electric vehicles," *IEEE Trans. Ind. Electron.*, vol. 64, no. 2, pp. 1404–1414, Feb. 2017.

[14] J. J. Eckert, L. C. de Alkmin e Silva, F. M. Santiciolli, E. dos Santos Costa, F. C. Corrêa, and F. G. Dedini, "Energy storage and control optimization for an electric vehicle," *Int. J. Energy Res.*, vol. 42, no. 11, pp. 3506–3523, Sep. 2018.

[15] J. Shen and A. Khaligh, "Design and real-time controller implementation for a battery-ultracapacitor hybrid energy storage system," *IEEE Trans. Ind. Informat.*, vol. 12, no. 5, pp. 1910–1918, Oct. 2016.

[16] J. Li, R. Xiong, H. Mu, B. Cornélusse, P. Vanderbemden, D. Ernst, and W. Yuan, "Design and real-time test of a hybrid energy storage system in the microgrid with the benefit of improving the battery lifetime," *Appl. Energy*, vol. 218, pp. 470–478, May 2018.

[17] R. Xiong, Y. Duan, J. Cao, and Q. Yu, "Battery and ultracapacitor in-the-loop approach to validate a real-time power management method for an all-climate electric vehicle," *Appl. Energy*, vol. 217, pp. 153–165, May 2018.

[18] A. Goussian, F.-A. LeBel, J. P. Trovão, and L. Boulon, "Passive hybrid energy storage system based on lithium-ion capacitor for an electric motor-cycle," *J. Energy Storage*, vol. 25, Oct. 2019, Art. no. 100884.

[19] J. Cao and A. Emadi, "A new battery/ultracapacitor hybrid energy storage system for electric, hybrid, and plug-in hybrid electric vehicles," *IEEE Trans. Power Electron.*, vol. 27, no. 1, pp. 122–132, Jan. 2012.

[20] A. Geetha and C. Subramani, "A comprehensive review on energy management strategies of hybrid energy storage system for electric vehicles," *Int. J. Energy Res.*, vol. 41, no. 13, pp. 1817–1834, Oct. 2017.

[21] C. Capasso, D. Lauria, and O. Veneri, "Experimental evaluation of model-based control strategies of sodium-nickel chloride battery plus supercapacitor hybrid storage systems for urban electric vehicles," *Appl. Energy*, vol. 228, pp. 2478–2489, Oct. 2018.

[22] Y. Wang, X. Li, L. Wang, and Z. Sun, "Multiple-grained velocity prediction and energy management strategy for hybrid propulsion systems," *J. Energy Storage*, vol. 26, Dec. 2019, Art. no. 100950.

[23] A. Castaings, W. Lhomme, R. Trigui, and A. Bouscayrol, "Comparison of energy management strategies of a battery/supercapacitors system for electric vehicle under real-time constraints," *Appl. Energy*, vol. 163, pp. 190–200, Feb. 2016.

[24] J. P. F. Trovao, V. D. N. Santos, C. H. Antunes, P. G. Pereirinha, and H. M. Jorge, "A real-time energy management architecture for multi-source electric vehicles," *IEEE Trans. Ind. Electron.*, vol. 62, no. 5, pp. 3223–3233, May 2015.

[25] J. Hu, X. Niu, X. Jiang, and G. Zu, "Energy management strategy based on driving pattern recognition for a dual-motor battery electric vehicle," *Int. J. Energy Res.*, vol. 43, no. 8, pp. 3346–3364, Jun. 2019.

[26] R. Hemmati, M. Shafie-Khah, and J. P. S. Catalao, "Three-level hybrid energy storage planning under uncertainty," *IEEE Trans. Ind. Electron.*, vol. 66, no. 3, pp. 2174–2184, Mar. 2019.

[27] B. Wang, J. Xu, D. Xu, and Z. Yan, "Implementation of an estimator-based adaptive sliding mode control strategy for a boost converter based battery/supercapacitor hybrid energy storage system in electric vehicles," *Energy Convers. Manage.*, vol. 151, pp. 562–572, Nov. 2017.

[28] R. Xiong, H. Chen, C. Wang, and F. Sun, "Towards a smarter hybrid energy storage system based on battery and ultracapacitor—A critical review on topology and energy management," *J. Cleaner Prod.*, vol. 202, pp. 1228–1240, Nov. 2018.

[29] W. Jiang, S. Xue, L. Zhang, W. Xu, K. Yu, W. Chen, and L. Zhang, "Flexible power distribution control in an asymmetrical-cascaded-multilevel-converter-based hybrid energy storage system," *IEEE Trans. Ind. Electron.*, vol. 65, no. 8, pp. 6150–6159, Aug. 2018.

[30] L. Zhang, X. Hu, Z. Wang, F. Sun, J. Deng, and D. G. Dorrell, "Multiobjective optimal sizing of hybrid energy storage system for electric vehicles," *IEEE Trans. Veh. Technol.*, vol. 67, no. 2, pp. 1027–1035, Feb. 2018.

[31] Q. Zhang, W. Deng, and G. Li, "Stochastic control of predictive power management for battery/supercapacitor hybrid energy storage systems of electric vehicles," *IEEE Trans. Ind. Informat.*, vol. 14, no. 7, pp. 3023–3030, Jul. 2018.

[32] J. P. Trovão, P. G. Pereirinha, H. M. Jorge, and C. H. Antunes, "A multi-level energy management system for multi-source electric vehicles—An integrated rule-based meta-heuristic approach," *Appl. Energy*, vol. 105, pp. 304–318, May 2013.

[33] D. Xu, J. Liu, X.-G. Yan, and W. Yan, "A novel adaptive neural network constrained control for a multi-area interconnected power system with hybrid energy storage," *IEEE Trans. Ind. Electron.*, vol. 65, no. 8, pp. 6625–6634, Aug. 2018.

[34] F. Zhou, F. Xiao, C. Chang, Y. Shao, and C. Song, "Adaptive model predictive control-based energy management for semi-active hybrid energy storage systems on electric vehicles," *Energies*, vol. 10, no. 7, p. 1063, Jul. 2017.

[35] S. Xie, X. Hu, S. Qi, and K. Lang, "An artificial neural network-enhanced energy management strategy for plug-in hybrid electric vehicles," *Energy*, vol. 163, pp. 837–848, Nov. 2018.

[36] B. Wang, C. H. Wang, Q. Hu, G. L. Ma, and J. H. Zhou, "Adaptive sliding mode control with enhanced optimal reaching law for boost converter based hybrid power sources in electric vehicles," *J. Power Electron.*, vol. 19, no. 2, pp. 549–559, 2019.

[37] A. Santucci, A. Sorniotti, and C. Lekakou, "Power split strategies for hybrid energy storage systems for vehicular applications," *J. Power Sources*, vol. 258, pp. 395–407, Jul. 2014.

BIN WANG was born in Guangxi, China, in 1987. He received the B.S. degree in automation engineering and the M.S. degree in control science and engineering from the Henan University of Science and Technology, Luoyang, China, in 2010 and 2013, respectively, and the Ph.D. degree in mechanical engineering from Xi'an Jiaotong University, Xi'an, China, in 2017. He is currently an Assistant Professor with the School of Mechanical Engineering, Xi'an Jiaotong University. His research interests include energy storage systems, electric vehicles, dc–dc converter control, and supercapacitor state-of-charge estimation.

QIAO HU was born in Hubei, China, in 1977. He received the Ph.D. degree from Xi'an Jiaotong University, Xi'an, China, in 2006. He is currently a Professor with the School of Mechanical Engineering, Xi'an Jiaotong University. His research interests include coordination control of underwater electric vehicles, underwater target intelligent detection and classification, automatic control, and fault diagnosis of mechatronic systems.

ZHIYU WANG was born in Sichuan, China, in 1996. He received the B.S. degree in information engineering from Xi'an Jiaotong University, Xi'an, China, in 2018. He is currently pursuing the master's degree in research at the School of Mechanical Engineering, Xi'an Jiaotong University. His research interests include supercapacitor state-of-charge estimation and electric vehicle energy management.

● ● ●